# A computer model for in-silico trials on pacemaker energy efficiency

Y. Coudière[1], M. Leguèbe[1], I. Balelli[2], A. Baretta[3], G. Fauré[4], D. Feuerstein[4]

[1] Univ. Bordeaux, CNRS, Inria, Bdx-INP, IMB, UMR 5251, IHU Liryc, F-33400 Talence, France
[2] Inria, Nice Sophia-Antipolis, France
[3] In Silico Trials, Italy
[4] Microport CRM, France

## Abstract

*Pacemakers are commonly required to treat bradycardias. They are composed of a pulse generator and leads implanted in the heart, and deliver an electrical pulse so as to elicit cardiac contraction. The capture threshold (minimum energy required to stimulate the heart) is critical to assess and predict pacemaker performance. Indeed, the threshold may change due to fibrosis associated with the inflammatory process, resulting in loss-of-capture, requiring re-hospitalization.*

*We developed a 3D model that computes threshold curves depending on the pacemaker and cardiac tissue properties. Its credibility is being assessed by verification and validation in the context of capture threshold measurements on animal hearts. It aims to assist device companies in the early development phase of new lead designs. Here, it is used to compute the proportion of a population for which the initial device setting no longer captures, based on user-defined lead geometric and electric properties and population statistics.*

*As a proof of concept, we compare the performance of MicroPort's VEGA™ lead and a custom one. The results show that the new design decreases the threshold to capture in one over three tested pulse durations, which is an improvement, but achieves poorer performance after the onset of fibrosis.*

## 1. Introduction

We are interested by bradycardia that require a permanent pacing protocol, following the guidelines [1] (Fig. 6 p e89). Permanent pacing requires an artificial pacemaker, a device composed of a pulse generator (electronics and battery), and leads which are implanted in the cardiac tissues. Theses bradycardia, related to sinus node diseases, are usually treated with a main lead implanted in the right ventricle. A pacemaker is a long-lasting device, whose management on a long term is crucial to actually treat the disease. Among other parameters, capture threshold, defined as the minimum energy required to stimulate the heart is a critical measurement to assess and predict the pacemaker performance at implantation and on the long term follow-up. Hence, capture threshold has to be accurately evaluated. Despite remarkable progress since its introduction, various complications may occur during the treatment, including changes in capture threshold, a known phenomenon with causes listed in [2]. It may result in loss of capture, a crucial problem for patients depending on the pacing function, and may require hospitalization and reprogramming of the device. Typical evolution of threshold to capture along time are reported in [3], where a plateau of the capture threshold is reached 16 weeks after implantation.

In this context, computational modeling may be used during the development phase of new devices, for several reasons, accelerating the development, reducing the resort to animal studies, etc. Here, we search for improved efficiency of the energy delivery of a new lead design with respect to a reference one. To this aim, we developed a computational model of the pulse generator and leads connection to a generic cardiac tissue through contact impedance, used to evaluate capture threshold curve [4]. Here, we use this model to study loss of capture due to changes in the cardiac tissue. We focus on changes associated to fibrosis, that are well documented (e.g. in [3]), so that they constitute a good compromise for evaluating the interest of in-silico models for pacemakers.

## 2. Formulation of the three-dimensional model

The model is written in a three-dimensional (3D) domain $\Omega$, split into the myocardium $\Omega_M$ and the blood bath $\Omega_B$. The lead has two metallic electrodes, a screw shaped one anchored in the myocardium named *tip*, and a distal one in the blood bath named *ring*. They are parts of the boundary of $\Omega$, noted $\Gamma_{\text{tip}}$ and $\Gamma_{\text{ring}}$. Capture is a local characterization of the excitability properties around the tip electrode, so that the domain $\Omega$ represents a small re-

gion of diameter 4 cm around the tip electrode, see fig. 1. The bidomain equations are written in $\Omega$,

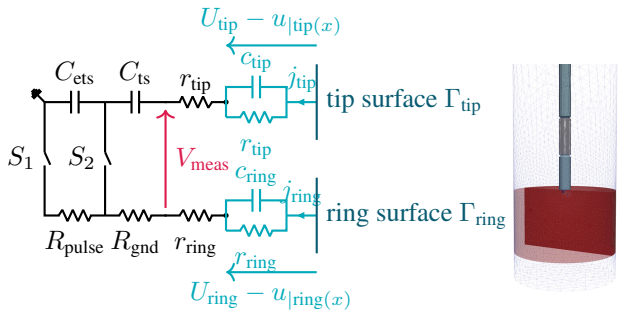


Figure 1: The principle of the 3D computational model used to compute threshold curves.

$$
\begin{aligned}
-\operatorname{div}(\sigma_i \nabla u_i) &= -c_m \partial_t v_m - I_{\text{ion}}(v_m, h) \quad \text{in } \Omega_M \\
-\operatorname{div}(\sigma \nabla u), &= \begin{cases} c_m \partial_t v_m + I_{\text{ion}}(v_m, h) & \text{in } \Omega_M, \\ 0 & \text{in } \Omega_B, \end{cases}
\end{aligned}
$$

with an ionic model, $\partial_t h + g_{\text{ion}}(v_m, h) = 0$ in $\Omega_M$. They are coupled to the equations of a pacemaker pulse generator, $\tau \frac{d}{dt} U_{\text{tip}} = U_{\text{ring}}$ during the electrical pulse, through impedance boundary conditions, see [4],

$$
-\sigma \nabla u \cdot n = c_{\text{e}} \partial_t (U_{\text{e}} - u_{|\Gamma_{\text{e}}}) + \frac{1}{r_{\text{e}}} (U_{\text{e}} - u_{|\Gamma_{\text{e}}}), \quad \text{on } \Gamma_{\text{e}}, \quad (1)
$$

where $\text{e} \in \{\text{tip}, \text{ring}\}$. The electrical potentials $U_{\text{tip}}$ and $U_{\text{ring}}$ in $\mathbb{R}$ are the potentials of the metallic electrodes. The pulse generator circuit is characterized by the time scale $\tau = RC$ where the resistance and capacitance depend on time (see [4], the stimulation has 3 stages), and the bioimpedances are modeled by parallel RC circuits, characterized by resistances $R_{\text{tip/ring}}$ and capacitances $C_{\text{tip/ring}}$.

The pulse is defined by its initial amplitude $U_{\text{tip},0}$ in V (charge of the capacitor at $t = 0$) and its duration $T$ in ms. Capture is detected by examining the activated volume $V_{40}(t) = |\{x \in \Omega : v_m(t, x) \geq -40\text{mV}\}|$. Since this volume is expected to increase for a supra-threshold stimulation and decrease otherwise, capture is detected if $V_{40}(T + t_1) < V_{40}(T + t_2)$ for $t_1 = 5\text{ms}$ and $t_2 = 10\text{ms}$.

## 3. Formulation of the in-silico trials, and computational pipeline

We are interested in the following question: *what are the changes of the energy delivery properties of a new pacemaker lead design, with respect to a reference one ?* It is addressed in the context of a population of persons who require a permanent pacemaker treatment for a sinus node disease [1]. We focus on people who would benefit from implantation of a bradycardia permanent pacemaker treatment with pacing lead in a healthy region of the right ventricle. Our objective is to evaluate the changes, and in particular to assess improvement, in the threshold to capture of a new, prospective, lead design with respect to an existing one. We would like, in particular, to evaluate how much the capture-threshold changes in the 16 weeks after implantation as described in [3].

*Primary objective* Our primary objective is to compare the proportion of the population for whom the initial setting of the device does not capture any more, i.e. who experienced loss-of-capture, due to fibrosis.

*Secondary objectives* Our secondary objective is to evaluate the changes in capture threshold after implantation due to fibrosis.

Using the capture detection computational model presented in section 2, the trial is designed and ran as follows.

The population is assumed to be initially homogeneous, all persons having the same capture properties, and is to have fibrosis after 16 weeks distributed according to a normal law (see below).

*First, the lead is assumed implanted in healthy tissue.* A threshold detection test is run with cardiac tissue parameters from the literature. Lead characteristics and a pulse duration $T$ are fixed, in practice through a user interface, see fig. 4. They are set within the range of values allowed by the pulse generator, and common in clinical practice. For this fixed pulse duration, the threshold is a voltage, searched in the decreasing order among a set of predefined values of the pulse generators: $\mathcal{R} = \{0.25, 0.50, 0.75, 1.00, 1.25, 1.50, 1.75, 2.00, 2.50, 3.00, 3.50, 4.00\}$ (in V), using the detection test from section 2. The search results in an interval $[V_-, V_+]$ between the last value to capture $V_+$ and the next one $V_-$ (in decreasing order). An additional safety factor is applied by assuming that *the pacemaker is tuned to the voltage value $V_\star$ just above $V_+$.*

*Second, fibrosis is assumed to have installed and stabilized*, so that the local conduction and excitation properties of the cardiac tissue are altered. We define a space-dependent parameter $\rho(x) \in [0, 1]$ that encodes the fibrosis level (0 no fibrosis, 1 maximum fibrosis): the electric conduction is lowered, and ionic currents are decreased down to 60% of their initial value [5], proportionally to the local fibrosis level. The fibrosis level is $\rho(x) = \frac{1}{2}(1 - \arctan(d(x) - d_h))$, where $d(x)$ is the distance to the tip electrode. It means that the fibrosis level decrease smoothly from the tip to the rest of the tissue, reaching 0.5 at the distance $d_h$, see fig. 2b. A typical value of the average distance $d_h$ is twice the radius of the tip lead.

This evolution is diverse and patient dependent, so that we expect the fibrosis level to be randomly distributed over the virtual population: *we assume that the half maximum distance $d_h$ follows a normal law: $d_h = \mathcal{N}(d_0, \sigma)$ of av-*

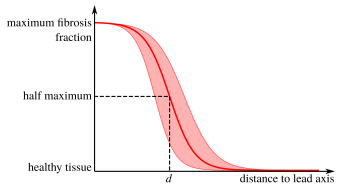


(a) Fibrosis level as a function of the distance to the tip. The average, second and third quartile of the population model are represented.

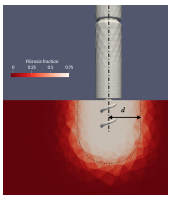

(b) Distribution of fibrosis (in level of white)

Figure 2: Characteristics of a sample test population.

*erage value $d_0$ and standard deviation $\sigma$*, see fig. 2a.

*The second step in the trial aims at measuring the fraction of the total population that undergoes loss of capture (primary objective).* This search amounts to compute capture thresholds for a wide range of the parameter $d_h$. We expect the capture threshold to decrease monotonically with respect to $d_h = \mathcal{N}(d_0, \sigma)$. Hence loss-of-capture is perfectly determined by a critical value $d_c$, such that loss of capture occurs only for $d > d_c$. The proportion of the population that undergoes loss-of-capture is then perfectly determined by the integral above $d_c$ of the distribution function associated to the normal law, see fig. 3.

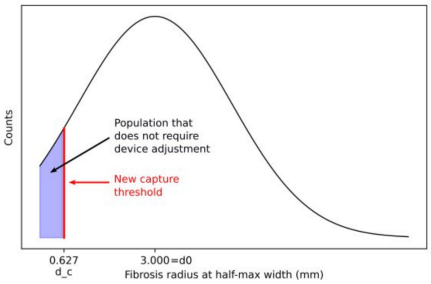


Figure 3: Example of computation of the proportion of population that requires adjustment of stimulation parameters. The shape of the population distribution is parametrized from the web platform.

## 4. Exemple results

The computations detailed in sections 2 and 3 are available through a web-based platform at InSilicoTrials Alessia, what do you want to write ?. A user chooses the lead geometrical and electrical bioimpedance parameters on a first page (shown on fig. 4) and then the pulse duration $T$ and the population parameters $d_0$ and $\sigma$ on a second page (all parameters are listed in table 1), and then run the computation. The inputs are processed as follows: generate a 3D mesh with the gmsh software[1]; detect the initial capture threshold $V_\star$ (first above $V_+$, before fibrosis); detect the critical value $d_c$ and compute the percentage of population that undergoes loss-of-capture. The last two steps are executed with our in-house software CEPS[2].

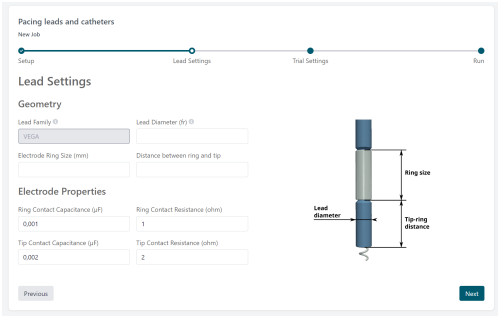


Figure 4: First page of the IST web-based platform.

| | Low | Up | Default |
|---|---|---|---|
| Diameter (mm) | 6.00 | 20.00 | 6.96 |
| $L_{\text{ring}}$ (mm) | 1.00 | 20.00 | 7.07 |
| Ring to Tip (mm) | 6.00 | 20.00 | 6.38 |
| $C_{\text{ring}}$ (µF) | $1 \times 10^{-5}$ | none | 5.55 |
| $R_{\text{ring}}$ (kΩ) | $1 \times 10^{-5}$ | none | 0.03 |
| $C_{\text{tip}}$ (µF) | $1 \times 10^{-5}$ | none | 18.74 |
| $R_{\text{tip}}$ (kΩ) | $1 \times 10^{-5}$ | none | 2.0 |
| Duration $T$ (ms) | 0.10 | 10.00 | 1.00 |
| $d_h$ (mm) | 0 | 2 | 1.0 |
| $\sigma$ (mm) | $1 \times 10^{-6}$ | | 1.0 |

Table 1: Parameters of a trial (defaults are from the Microport VEGA lead and bench experiments).

We first ran the pipeline with the original design of the Microport VEGA lead, and with pulse duration $T = 0.25$, 0.5 and 1 ms. The voltage thresholds (upper bound $V_+$) were found at 2, 1.25 and 0.75 V, respectively (fig. 5). Therefore, the voltages used to find the fibrosis thresholds were $V_\star = 2.5$, 1.5 and 1 V, respectively, with results for $d_c$ compiled in fig. 6.

We then ran the pipeline with the same stimulation parameters ($T \in \{0.25, 0.5.1\}$ ms) and electrode contact properties for a second, different geometrical design of the lead, called *custom*, with lead diameter decreased from 7 to 6 mm, and ring electrode size decreased from 7 to 2.5 mm. The results are reported in fig. 5 and 6 for comparison with the reference lead.

The percentages of population that does not undergo loss-of-capture, i.e. for whom the initial settings $T$ and $V_\star$ still trigger action potentials are reported in table 2.

The results in fig 5 show that, right after implantation in a healthy tissue, the threshold to capture for the custom lead is decreased for a pulse duration of 0.5 ms (1.50 to 1.25 V), but increased for the other two tested durations, 0.25 ms (2.5 to 3 V) and 1 ms (1 to 1.25 V). Decrease in threshold to capture is an improvement that we look for.

[1] http://gmsh.info/

[2] https://carmen.gitlabpages.inria.fr/ceps/

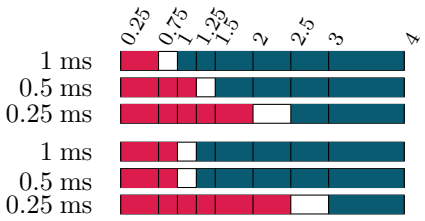


Figure 5: Initial threshold detection. The threshold is between green (capture) and red (no capture).

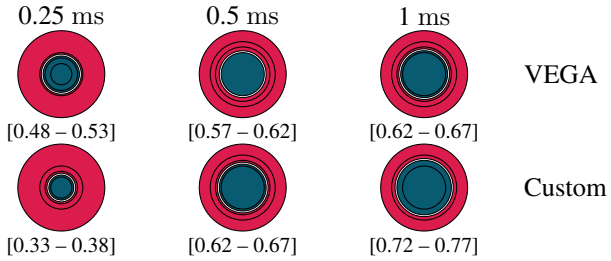


Figure 6: Fibrosis radius (intervals are in $\mathrm{mm}$) that allows capture (green) or not (red) with pulse settings $T$ and $V_\star$ from fig. 5.

| Fibrosis law $\mathcal{N}(d_h, \sigma)$ | | VEGA | | |
|---|---|---|---|---|
| $d$ | $\sigma$ | 0.25ms | 0.5ms | 1.0ms |
| 3.0 | 2.0 | 3.92 % | 4.87 % | 5.36 % |
| 0.0 | 0.5 | 77.37 % | 82.19 % | 86.21 % |
| Fibrosis law $\mathcal{N}(d_h, \sigma)$ | | Custom | | |
| $d$ | $\sigma$ | 0.25ms | 0.5ms | 1.0ms |
| 3.0 | 2.0 | 2.61 % | 5.36 % | 6.40 % |
| 0.0 | 0.5 | 51.47 % | 75.34 % | 84.79 % |

Table 2: Percentages of population for which the pacemaker still captures.

Our primary objective is answered by table 2. It shows two situations. First, if the average extend of fibrosis is 0 with a small standard deviation of 0.5 $\mathrm{mm}$, then for the VEGA lead, 77 % to 86 % of the population remains in capture range after fibrosis has installed permanently. In comparison, these numbers are 51 % to 84 % for the custom lead, meaning that the custom lead achieves poorer performance. Second, if the average extend of fibrosis is large (3 $\mathrm{mm}$) with a large standard deviation (2 $\mathrm{mm}$), then in any case only a very small fraction of the population remains in the capture range, 4 % to 5 % for the VEGA lead, and 2 % to 6 % for the custom lead. Anyway, in this case, the custom lead improves the performance for pulse durations of 0.5 $\mathrm{ms}$ and 1 $\mathrm{ms}$ (resp. 4.87 % to 5.36 %, and 5.36 % to 6.40 %).

Our secondary objective is addressed through fig. 6. The results are consistent with the ones from the primary objective: the extend of fibrosis for which loss-of-capture occurs increased for pulse durations of 0.5 and 1 $\mathrm{ms}$, and decreased at 0.25 $\mathrm{ms}$.

## 5. Conclusion

In parallel of this study, the credibility of the model is assessed following the verification and validation framework [6].As compared to this framework, the trial presented here relies on a few more assumptions: implantation sites are supposed to be all identical and healthy, the tip fibrosis has been simplified to an axi-symmetric region, and characterized by its extent only.

This may be far from the clinical reality, although it is a proof of concept of in-silico trials, that allows tractable computations with our model, in terms of CPU complexity. It may be extended to establish a computational model that remains robust and reflects better the lead placement in real tissue, and associated electrical energy delivery. A more general population could be considered, that would have diverse tissue properties at the implantation siteAnother possible generalization would be to use the model to study the loss-of-capture due to connection issues with the device.

## Acknowledgments

This study received funding from the European Research Council under the Horizon 2020 RIA program, grant agreement N°101078351, and support from the French Government, grant ANR-10-IAHU-04.

## References

[1] Kusumoto FM, et al. 2018 ACC/AHA/HRS guideline on the evaluation and management of patients with bradycardia and cardiac conduction delay. JACC 2019;74(7):e51–e156.

[2] Sabbagh E, et al. Causes of failure to capture in pacemakers and implantable cardioverter-defibrillators. Journal of Innovations in Cardiac Rhythm Management February 2020; 11(2):4013–4017.

[3] Mond HG, Helland JR, Stokes K, Bornzin GA, McVenes R. The electrode - tissue interface: The revolutionary role of steroid - elution. Pacing and Clinical Electrophysiology 2014;37(9):1232–1249.

[4] Pannetier V, et al. Modeling cardiac stimulation by a pacemaker, with accurate tissue-electrode interface. In FIMH. Springer Nature, 2023; 194–203.

[5] Arevalo HJ, et al. Arrhythmia risk stratification of patients after myocardial infarction using personalized heart models. Nature Communications 2016;7(1).

[6] 40-2018 AV. Assessing credibility of computational modeling through verification and validation: Application to medical devices, 2018.

Address for correspondence:

Yves Coudière
Inria, 200 avenue de la vielle tour, 33405 Talence Cedex
yves.coudiere@u-bordeaux.fr